An Integrated Reaction-Transport Model for DNA Surface Hybridization: Implications for DNA Microarrays

RAGHVENDRA SINGH,[1] JOHANNES NITSCHE,[1] and STELIOS T. ANDREADIS[1,2]

[1]Bioengineering Laboratory, 908 Furnas Hall, Department of Chemical and Biological Engineering, University at Buffalo, State University of New York, Amherst, NY 14260-4200, USA; and [2]Center of Excellence in Bioinformatics and Life Sciences, Buffalo, NY 14203, USA

Abstract—DNA microarrays have the potential to revolutionize medical diagnostics and development of individualized medical treatments. However, accurate quantification of scantily expressed genes and precise measurement of small differences between different treatments is not currently feasible. A major challenge remains the understanding of physicochemical processes and rate-limiting steps of hybridization of complex mixtures of DNA targets on immobilized DNA probes. To this end, we developed a mathematical model to describe the effects of molecular orientation and transport on the kinetics and efficiency of hybridization. First, we calculated the hybridization rate constant based on the distance between the complementary nucleotides of the target and probe DNA. The surface reaction rate was then integrated with translational and rotational transport of target DNA to the surface to calculate the kinetics of hybridization. Our model predicts that hybridization of short DNA targets is diffusion limited but long targets are kinetically limited. In addition, for DNA targets with wide size distribution, it may be difficult to distinguish between specific binding of long targets from nonspecific binding of short ones. Our model provides novel insight into the process of DNA hybridization and suggests operating conditions to improve the sensitivity and accuracy of microarray experiments.

Keywords—Reaction-diffusion model, DNA, Hybridization, Nucleic acid, Rotational diffusion, Kinetics.

INTRODUCTION

Nucleic acid hybridization has been employed in a wide variety of biological assays including Southern blot, Northern blot, and *in situ* hybridization. More recently, DNA hybridization on solid surfaces has been used to develop microarray technologies for simultaneous quantitation of large numbers of genes.[10,24] DNA microarrays have been used to address many biological problems including cell cycle and metabolism of yeast cells,[18,31,49,50,54] response of human fibroblasts to serum,[28] development of central nervous system,[59] differentiation of hematopoietic cells,[52] branching morphogenesis of the collecting system of the kidney,[43] progression and classification of human cancers,[16,19,23,37,44] and development of engineered tissues such as muscle and skin.[29,30,32] This technology has transformed our way of thinking about biological systems as complicated molecular networks and established databases that may be useful in reaching a global understanding of biological processes.[17,41,47]

Microarray experiments explore complex biological processes such as tissue development and disease progression by identifying the wiring of genetic networks that regulate the observed tissue phenotype. To this end, quantitative measurement of gene expression is required to draw reliable conclusions on individual genes or gene networks that are modulated in response to a range of environmental stimuli or therapeutic treatments. However, a number of laboratories reported large variability of gene expression between different probes in the same array, which in some cases was higher than interarray variability.[33,61] Statistical models have attempted to address this problem by using empirical correlations that best fit the experimental data.[1,27,33] Even though statistical correlations may help the analysis of microarray data, they are not based on physical principles and therefore, they cannot provide physical insight into the process of DNA hybridization. A fundamental understanding of the physicochemical processes that take place during surface hybridization is necessary to design more efficient and selective microarray devices that provide quantitative and reliable gene expression data.

Experimental studies examined several physicochemical aspects of DNA hybridization including

Address correspondence to Stelios T. Andreadis, Bioengineering Laboratory, 908 Furnas Hall, Department of Chemical and Biological Engineering, University at Buffalo, State University of New York, Amherst, NY 14260-4200, USA. Electronic mail: sandread@eng.buffalo.edu

various methods for DNA surface immobilization and effects of DNA surface density on the kinetics of hybridization.[34,45,51] The rate of surface hybridization has also been used to distinguish specific from non-specific binding and even determine single nucleotide mismatches between target and probe sequences.[15,46] These studies showed that the kinetics of hybridization on surface-immobilized DNA is different from the solution-phase reaction and can not be explained by the effects of DNA surface density alone.[46] Therefore, there is a need for a comprehensive theoretical approach to understand this process from first principles.

Several theoretical studies provided considerable insight into the process of surface DNA hybridization.[15,26,51,57] In one of the first studies, Wang *et al.* assumed that hybridization occurred by either of two mechanisms: direct binding from solution or nonspecific adsorption followed by subsequent surface diffusion of target to immobilized DNA.[11] An integral assumption was that the bulk concentration of target DNA remained constant during hybridization, a condition that is valid only for early time points before binding depletes the targets in close proximity to the surface. This work was recently extended to include an explicit description of bulk and surface diffusion to calculate the probability of binding as a function of time.[20] Pappaert *et al.* employed a stochastic model that accounted only for diffusion perpendicular to the surface and provided useful insight on the effects of fluid thickness and mixing on the rate of hybridization.[39] They showed that hybridization is limited by the rate of reaction at early times when the target DNA concentration in the bulk remains high but becomes diffusion limited at later times when the target DNA is depleted in the volume immediately adjacent to the surface. Based on this data the authors designed microfluidic and shear-driven flow devices to improve the sensitivity and accuracy of microarrays by overcoming the diffusion limitations of surface reaction.[38,40] A more recent study by Gadgil *et al.* used a reaction–diffusion model that was solved for small sample volume and gap height (20 μL and 140 μm, respectively) and for large target DNA with average length of 2000 nucleotides.[21] Their results showed that only DNA close to the surface hybridized and that the bulk concentration at a distance of 250 μm or longer remained unchanged for as long as 12 h. Interestingly, the model also predicted that the intensity of hybridized targets best reflects their concentration in solution when the reaction is far from equilibrium.

Despite these recent advances, some important physical aspects such as rotational diffusion of target DNA and orientation of the reactive site at the time of collision have been neglected in surface hybridization models. Two DNA strands hybridize only when a small number of reactive nucleotides (~20 bases) on the target are positioned in close proximity and in anti-parallel orientation to their complementary counter-parts on the probe. Therefore, only a small fraction of target molecules with the correct orientation would bind to the immobilized probes at any given moment.

The present study is undertaken to provide a comprehensive mathematical model of surface hybridization including rotational diffusion of target DNA and orientation-dependent reaction probability. The kinetics of hybridization is calculated based on the physical distance between complementary nucleotides of target and probe DNAs, ultimately providing a surface reaction rate constant that is a strong function of molecular orientation. The kinetics is then incorporated into a reaction–diffusion model that accounts for both rotational and translational diffusion of target DNA and calculates the fraction of hybridized targets as a function of time. Our model provides insight into the effect of target DNA orientation and size on the hybridization rate and suggests ways to improve the accuracy and sensitivity of microarray-based genetic analysis.

MODEL FORMULATION

Figure 1 presents the idealized model used here to describe the hybridization process, which occurs in an aqueous layer of thickness h. The bottom surface with immobilized probe DNA coincides with the plane $z = 0$ in space-fixed coordinates (x, y, z). This surface is modeled as a periodic array of square unit cells of side length L numbered with a pair of indices (j, k). Each contains a single probe DNA molecule comprising N_r nucleotides distinguished by an index $i = 1, 2, \ldots, N_r$. The internucleotide distance, denoted by s, is estimated to be 3.4 Å.[42] The probe molecule is aligned with the y axis and positioned such that its central nucleotide coincides with the center of the unit cell (if N_r is even, the central nucleotide is taken to be the $[(N_r + 2)/2]$th, and lies at a distance $s/2$ from the geometric midpoint of the DNA strand) (Figs. 1b, c). The triple of coordinates $\vec{u}_{ijk}$ of nucleotide i within unit cell (j, k) on the surface (Fig. 1b) is given by

$$\vec{u}_{ijk} = (jL, kL - [(N_r + 1)/2 - i]s, 0) \quad (N_r \text{ odd}),$$
$$= (jL, \ kL - [(N_r + 2)/2 - i]s, \ 0) \quad (N_r \text{ even})$$

$$(1)$$

For definiteness, the side length L is taken to be 100 Å in the illustrative calculations ultimately reported, corresponding to a probe density of 10^{12} molecules per cm^2, but this geometrical parameter can

(a)

Globular DNA

Hydrodynamic core

r_h

r_g

Reactive spot

Target DNA

(b)

z

z'

(x_0, y_0, z_0)

x'

y'

$(0^{th}, 0^{th})$ cell

x

y

(c)

z

kL

x

y

$(i = 1)$

jL

(j^{th}, k^{th}) cell

$(i = Nr)$
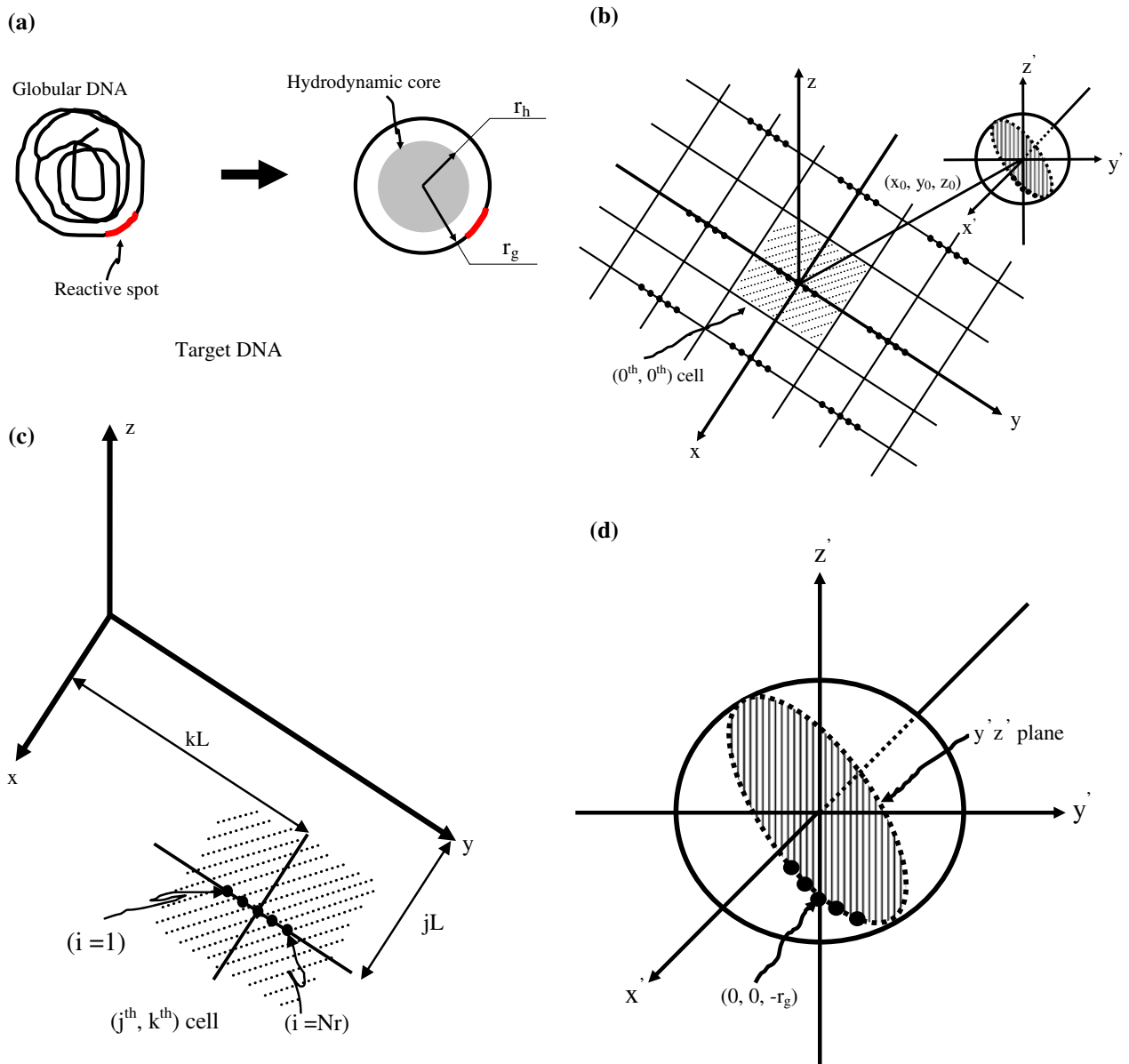
(d)

z'

$y'z'$ plane

y'

x'

$(0, 0, -r_g)$

FIGURE 1. Definition sketch. (a) Approximation of a globular target DNA with a spherical particle with radius of gyration, r_g, and hydrodynamic radius, r_h. (b) Overall view of surface with periodically distributed immobilized DNA probes and a globular DNA target in solution. (c) Notational details for the probe DNA molecule in unit cell (j, k) on the surface. (d) Notational details for a target DNA molecule, referred to target-fixed coordinates x', y', z'.

be varied to reflect changes in the density of immobilized DNA.

Previous experimental work showed that a 200-nucleotide or longer DNA molecule assumes globular conformation in solution[53] and therefore, it can be approximated by a soft sphere of radius, r_g (radius of gyration), which correlates with the total number of nucleotides N and surrounds a hydrodynamic core of radius, r_h (hydrodynamic radius) (Fig. 1a). Experimental values of the radius of gyration r_g of DNA molecules with various total numbers of nucleotides N

are available in the literature[53] and the hydrodynamic radius can be calculated using the Einstein–Stokes equation (Eq. 14). Cartesian coordinates (x', y', z') fixed on the target (Fig. 1d) serve to define its surface structure, which comprises N_r reactive nucleotides complementary to the nucleotides of each probe DNA molecule on the surface, likewise distinguished by the integer $i = 1, 2, \ldots, N_r$. They are spaced evenly along the circular arc defined by the $y'z'$ plane. With respect to the target-fixed coordinate system, the triple of coordinates $\vec{v}_1'$ of nucleotide i is given by

$$\vec{v}_i' = \left(0, \, r_{\mathrm{g}} \sin(\ell_i/r_{\mathrm{g}}), \, -r_{\mathrm{g}} \cos(\ell_i/r_{\mathrm{g}})\right),$$
$$\text{where } \ell_i = -[(N_r + 1)/2 - i]s \quad (N_r \text{ odd}), \quad (2)$$
$$= -[(N_r + 2)/2 - i]s \quad (N_r \text{ even}).$$

The state of a target DNA molecule is defined by the triple of position coordinates $\vec{x}_0 = (x_0, y_0, z_0)$ of its center measured with respect to the space-fixed axes x, y, z, and by a triple of Eulerian angles θ, ϕ, and ψ giving the directions of the axes x', y', z' relative to x, y, z. According to the convention adopted here,[2,60] the angles θ and ϕ specify the direction of the z' axis following the usual definition of polar and azimuthal angles, respectively, in spherical coordinates,[4] and ψ specifies the amount of twist about this axis (other conventions also exist[22]). With respect to the space-fixed (x, y, z) coordinate system, the triple of coordinates $\vec{v}_i$ of nucleotide i is given by the well-known transformation

$$\vec{v}_i = \vec{x}_0 + R\vec{v}_i' \qquad (3)$$

involving the rigid-body rotation matrix:

$$R = \begin{bmatrix} \cos\theta\cos\phi\cos\psi - \sin\phi\sin\psi & -\cos\theta\cos\phi\sin\psi - \sin\phi\cos\psi & \sin\theta\cos\phi \\ \cos\theta\sin\phi\cos\psi + \cos\phi\sin\psi & -\cos\theta\sin\phi\sin\psi + \cos\phi\cos\psi & \sin\theta\sin\phi \\ -\sin\theta\cos\psi & \sin\theta\sin\psi & \cos\theta \end{bmatrix} \qquad (4)$$

Here the apposition of R and $\vec{v}_i'$ implies matrix-vector multiplication.

Reaction of the target DNA with any probe DNA can occur once diffusion has brought the target into contact with the surface (i.e., to a configuration with $z_0 = r_{\mathrm{g}}$). The probability of a successful binding reaction clearly depends critically upon the distances between complementary nucleotides at the contact configuration. Reaction is likely only if the reactive site of the target DNA (comprising the linear sequence of nucleotides $i = 1, 2, \ldots, N_r$) is very nearly anti-parallel to the reactive site of the probe DNA, so that the $5' \to 3'$ sequence anneals with the $3' \to 5'$ sequence. A good measure of the degree of alignment can be formulated in terms of the distance

$$d_{ijk} = d_{ijk}(x_0, y_0, z_0, \theta, \phi, \psi) = |\vec{v}_i - \vec{u}_{ijk}| \qquad (5)$$

between reactive nucleotide i on the target and its complement in a unit cell (j,k) on the surface. This distance is strongly dependent upon the configuration of the target DNA molecule given by the position

coordinates (x_0, y_0, z_0) of its center and the triple of Eulerian angles (θ, ϕ, ψ). Although d_{ijk} has significance as a geometrical quantity for all configurations, its pertinence to binding is restricted to configurations for which $z_0 = r_{\mathrm{g}}$.

Note that the model assumes that the DNA is spherical and that the patch is on the surface of the sphere. Molecular orientations in which the reactive patch may be buried inside the sphere are not explicitly accounted in the model. From a practical standpoint, these orientations would reduce the affinity for the probe considerably and a different probe (absorbed oligonucleotide) should be designed that would bind to a reactive site on the surface of the sphere.

Kinetic Model

A good indicator of the degree of alignment between reactive sites when the target is touching the surface $(z_0 = r_{\mathrm{g}})$ is the average distance between complementary nucleotides in the target and probe DNA, defined as:

$$d_{jk} = d_{jk}(x_0, y_0, \theta, \phi, \psi) = \frac{\displaystyle\sum_{i=1}^{N_r} d_{ijk}(x_0, y_0, r_{\mathrm{g}}, \theta, \phi, \psi)}{N_r} \qquad (6)$$

The mean distance is small for configurations providing something close to the optimal alignment between reactive sites, and large for grossly misaligned configurations. As a model of site-specific reactivity, we introduce a configuration-dependent binding rate constant given by

$$k_{\mathrm{config}}(x_0, y_0, \theta, \phi, \psi) = k_0 \sum_{j=-m/2}^{m/2} \sum_{k=-n/2}^{n/2} \exp\left(-d_{jk}/d_0\right), \qquad (7)$$

where d_0 is a tolerance parameter quantifying how close complementary nucleotides must be in order to have a significant probability of binding. Equation (7)

has the features that: (i) the rate constant declines sharply with small deviations from the perfectly matching configuration; and (ii) the neighboring probes also contribute to the rate constant. To resolve configurational effects at the level of single nucleotides, we used for d_0 a value that is half the internucleotide distance: $d_0 = s/2 = (1.7 \text{ Å})$. The coefficient k_0 is an empirical factor that reflects the overall binding affinity between the two reactive nucleotide sequences when they are properly aligned. It may account for the dependence of the binding reaction rate on temperature, salt concentration, and chemical composition, e.g., G-C content of the reactive site. The choice of an exponential function in Eq. (7) is arbitrary but reasonable, and it captures the strong dependence of the reaction rate constant on the distance between complementary nucleotides. For a target DNA molecule approaching the surface above the (0,0)th unit cell ($j = k = 0$), interactions with the surface are dominated by the interaction with the probe DNA in this unit cell. Interactions with probe DNAs in neighboring unit cells also occur, although they are weaker given the greater internucleotide separations involved. The summation over j and k in Eq. (7) accounts for all interactions between the approaching target DNA and probe DNAs on the surface. For the small value $d_0 = s/2$ used, test calculations show that only the closest ten neighbors or fewer in the x and y directions contribute significantly to the value of k_{config}. Thus the summation is truncated at $m = n = 10$.

The angular coordinate most decisive in determining the binding reactivity at contact is θ, because it controls whether or not the reactive site presented by the target DNA faces the surface. Our calculations (see Results below) confirm that changes in ϕ and ψ generally do not alter k_{config} as dramatically as changes in θ. The coefficient k_{config} also varies with x_0 and y_0, which control the relative positions of the complementary nucleotide sequences. As a first approximation, made in the interest of reducing the number of configurational coordinates involved in the subsequent diffusion problem, we: (i) average k_{config} over the ϕ and ψ coordinates; and (ii) also average k_{config} over x_0 and y_0, thereby treating the actual surface (whose binding reactivity is concentrated around the immobilized probe nucleotide sequences) as a homogeneously reactive surface characterized by a spatially averaged rate coefficient. The average over the whole surface is equivalent to the average over a single unit cell in the target DNA's position coordinates x_0 and y_0, given the assumed spatially periodic surface distribution. Thus, we consider the simpler situation of configuration-specific reactivity at contact ($z_0 = r_g$) described by the averaged rate coefficient:

$$k(\theta) = \frac{\int\limits_{-L/2}^{L/2} \int\limits_{-L/2}^{L/2} \int\limits_{0}^{2\pi} \int\limits_{0}^{2\pi} k_{\text{config}}(x_0, y_0, \theta, \phi, \psi) d\psi \, d\phi \, dx_0 \, dy_0}{\int\limits_{-L/2}^{L/2} \int\limits_{-L/2}^{L/2} \int\limits_{0}^{2\pi} \int\limits_{0}^{2\pi} d\psi \, d\phi \, dx_0 \, dy_0} \tag{8}$$

Dynamics of Diffusion and Surface Reaction

The average embodied in Eq. (8) effectively reduces the set of variables describing the state of a DNA molecule to a single angular coordinate (the polar angle θ) in addition to the elevation z_0 of its center. The distribution over configurations (z_0, θ) is described by a distribution function $P(z_0, \theta)$ having the significance that $P(z_0, \theta) \sin\theta \, dz_0 \, d\theta$ is the number of moles of DNA per area (considered parallel to the xy plane) with centers lying between elevations z_0 and $z_0 + dz_0$ and polar angles having values between θ and $\theta + d\theta$. The ordinary concentration $C(z_0)$ (moles per unit volume) is just the configurational distribution without regard to molecular orientation, i.e., $C(z_0) = \int_0^\pi P(z_0, \theta) \sin\theta d\theta$. For a hypothetical solution at concentration C of molecules evenly distributed (unbiased) over all orientations, P would simply be equal to $(1/2)C$. In the hybridization process, P in fact varies with both z (because diffusion to the surface is driven by a vertical concentration gradient) and θ (because molecular orientations near the ones for which $k(\theta)$ is high are selectively depleted by the binding reaction).

The distribution P is governed by a diffusion equation containing terms describing both translational and rotational diffusion, respectively characterized by a translational diffusion coefficient $D(z_0)$ and a rotational diffusion coefficient D_r[8,9,13,36]:

$$\frac{\partial P}{\partial t} = \frac{\partial}{\partial z_0}\left(D(z_0)\frac{\partial P}{\partial z_0}\right) + \frac{D_r}{\sin\theta}\frac{\partial}{\partial\theta}\left(\sin\theta\frac{\partial P}{\partial\theta}\right) \tag{9}$$

Translational diffusion delivers target DNA molecules to the surface, and rotational diffusion alters their orientation. Both processes act in concert in bringing the reactive sites to a state compatible with a high probability of reaction. The transport equation (9) is supplemented with initial and boundary conditions reflecting physical realities of the hybridization process:

$$P(z_0, 0) = P_0 \equiv (1/2)C_0, \tag{10}$$

$$D(r_g)\frac{\partial P(r_g, \theta, t)}{\partial z_0} = k(\theta)P(r_g, \theta, t) \tag{11}$$

$$D(h)\frac{\partial P(h, \theta, t)}{\partial z_0} = 0, \tag{12}$$

$$P \text{ and } \frac{\partial P}{\partial \theta} \text{ bounded at } \theta = 0 \text{ and } \theta = \pi \qquad (13)$$

The initial condition (Eq. 10) states that the experiment starts with the aqueous layer uniformly filled (spatially well mixed and orientationally randomized) with target DNA at concentration C_0. The boundary condition (Eq. 11) equates the flux of target DNA delivered to the surface by diffusion with the rate (moles per area per time) of binding at the surface; target–surface contact occurs for $z_0 = r_g$, and binding is described by an assumed first-order rate expression incorporating the orientation-dependent coefficient $k(\theta)$. The boundary condition (Eq. 12) expresses the fact that no target DNA passes through the air–liquid interface (zero flux) at the top of the solution ($z = h$). The boundedness conditions (Eq. 13) are of the usual type imposed at $\theta = 0$ and $\theta = \pi$ for problems with a polar angular coordinate.[58]

Far from the surface the diffusivity $D(z)$ for translational motion perpendicular to the surface equals the bulk aqueous diffusivity D_∞, given by the Stokes–Einstein relation

$$D_\infty = \frac{k_B T}{6\pi\mu r_h}, \qquad (14)$$

in which μ is the viscosity of the aqueous medium, and r_h is the effective hydrodynamic radius of the DNA molecule. The diffusivity $D(z_0)$ decreases with decreasing z because of a well-known hydrodynamic wall effect,[6,25] as described by the equation:

$$D(z) = \frac{D_\infty}{\lambda(z)}, \qquad (15)$$

in which $\lambda(z)$ is the increased drag factor tabulated, e.g., by Brenner.[6] Theoretically, for perfectly smooth spherical and planar surfaces, $D(z) \to 0$ ($\lambda(z) \to \infty$) as $z \to r_h$ owing to the lubrication singularity,[12] which would preclude target–surface contact and binding in any finite time. However, molecular surfaces are not perfectly smooth and would not actually give rise to a lubrication singularity. We account for this fact by allowing the effective hydrodynamic core of the DNA molecule to lie a little inside the sphere representing its effective hard-sphere surface, i.e., by taking $r_g > r_h$. Thus, $D(z)$ would be substantially reduced from D_∞ but nonzero at $z = r_g$. We approximate $\lambda(z)$ by the asymptotic expression[6,25]:

$$\lambda(z) \sim 1 + \frac{9}{8}\frac{r_h}{z}. \qquad (16)$$

This formula, which is valid as an asymptotic result for $z \gg r_h$, offers a reasonable quantitative approximation to exact values of $\lambda(z)$ for elevations z of the order of target radius r_g, and remains finite at $z = r_g$.

Experimental values of the bulk diffusivity of DNA, D_∞[53] yield the effective (Stokes–Einstein equivalent) radius r_h of the target molecule via Eq. (14). This radius is then used to calculate its rotational diffusivity D_r via the corresponding Stokes–Einstein relation[7]:

$$D_r = \frac{k_B T}{8\pi\mu r_h^3}. \qquad (17)$$

Close to the surface where reaction occurs, the orientation of target DNA determines the probability of a successful collision between the target and probe DNA molecules, and the distribution of DNA molecules has a strong angular dependence. In contrast, far from the surface the distribution over molecular orientations relaxes to a uniform angular distribution, so that only spatial gradients exist. Consequently, the transport problem can be divided in two zones: a microscopic zone comprising the first few molecular diameters above the surface (where both rotational and translational diffusion are important), and the bulk of the fluid further above (where only translation diffusion is important).

Microscopic Problem

In the thin layer close to the surface, the flux to the surface equals the rate of reaction, which depends on the orientation of the target DNA. In this zone, loss of DNA from solution due to hybridization is compensated by a constant flux of DNA molecules down from the bulk (driven by a limiting concentration gradient β far above the surface relative to the molecular diameter), thus maintaining the compartment at pseudo-steady state. Accordingly, the governing equation and boundary conditions are as follows:

$$\frac{\partial}{\partial z_0}\left(D(z_0)\frac{\partial C}{\partial z_0}\right) + \frac{D_r}{\sin\theta}\frac{\partial}{\partial \theta}\left(\sin\theta\frac{\partial C}{\partial \theta}\right) = 0; \qquad (18)$$

$$B.C.1: \quad z_0 = r_g: \quad D(r_g)\frac{\partial C(r_g,\theta)}{\partial z_0} = k(\theta)C(r_g,\theta); \qquad (19)$$

$$B.C.2: \quad z_0 \to \infty: \quad \frac{\partial C(\infty,\theta)}{\partial z} \to \beta; \qquad (20)$$

$$B.C.3\&4: \quad \theta = 0,\pi: \quad C \text{ and } \frac{\partial C}{\partial \theta} \text{ bounded.} \qquad (21)$$

The preceding microscopic equations are actually solved in the dimensionless form:

$$\left(\frac{1}{1+\frac{9\rho}{8\eta}}\right)\frac{\partial^2\xi}{\partial\eta^2} + \left(\frac{72\rho}{(8\eta+9\rho)^2}\right)\frac{\partial\xi}{\partial\eta} + \gamma\frac{\partial^2\xi}{\partial\theta^2}$$
$$+ \left(\frac{\gamma}{\tan\theta}\right)\frac{\partial\xi}{\partial\theta} = 0, \qquad (22)$$

$$\left(\frac{1}{1+\left(\frac{9\rho}{8}\right)}\right)\frac{\partial\xi}{\partial\eta}(1,\theta) = Da(\theta)\xi(1,\theta), \qquad (23)$$

$$\lim_{\eta\to\infty}\frac{\partial\xi}{\partial\eta}(\eta,\theta) = 1, \qquad (24)$$

$$\frac{\partial\xi}{\partial\theta}(\eta,0) = 0, \qquad (25)$$

$$\frac{\partial\xi}{\partial\theta}(\eta,\pi) = 0, \qquad (26)$$

where

$$\xi = \frac{C}{\beta r_{\mathrm{g}}}; \quad \eta = \frac{z}{r_{\mathrm{g}}}; \quad \rho = \frac{r_{\mathrm{h}}}{r_{\mathrm{g}}}; \quad \gamma = \frac{D_{\mathrm{r}}r_{\mathrm{g}}^2}{D_\infty}; \quad Da(\theta) = \frac{k(\theta)r_{\mathrm{g}}}{D_\infty}. \qquad (27)$$

$Da(\theta)$ is an orientation-dependent Damköhler number, which is a ratio of rate of reaction on the surface to the rate of diffusion to the surface.

Solution of the microscopic problem provides the concentration of DNA as a function of molecular position (elevation of the center above the surface, z_0) and orientation (angular coordinate θ). From this information we can calculate the limiting ($z_0 \gg r_{\mathrm{g}}$ or $\eta \gg 1$) DNA flux toward the surface (at locations far above it relative to the molecular diameter, but close to it in macroscopic terms). This flux can be quantified in terms of an effective average surface reaction rate coefficient, $\overline{k}$, encapsulating the overall outcome of the orientation-dependent diffusion and reaction process occurring near the surface. The average rate constant, $\overline{k}$ is then used in a reactive surface boundary condition in the time-dependent problem in the bulk fluid to calculate the observable kinetics of surface hybridization. For more details on the calculation of $\overline{k}$ from the solution of the microscopic problem, see Appendix A.

Macroscopic Problem

Far from the surface rotational diffusion is not important, and the problem can be simplified to a time-dependent one-dimensional diffusion equation with reaction at the boundary. Although the DNA target molecules still undergo Brownian motion in the x–y plane, the concentration gradient is generated in the z-direction, perpendicular to the surface where the target DNA is consumed—assuming that probe DNA is immobilized only on the surface and not the walls of the hybridization chamber. Surface DNA hybridization is accounted for in the boundary conditions and modeled as a first-order reaction with rate constant $\overline{k}$, as calculated from the microscopic model:

$$\frac{\partial C}{\partial t} = D_\infty\frac{\partial^2 C}{\partial z^2}, \qquad (28)$$

$$I.C.: \quad C(z,0) = C_0, \qquad (29)$$

$$B.C.1: \quad z = 0: \quad D_\infty\frac{\partial C(0,t)}{\partial z} = \overline{k}C(0,t), \qquad (30)$$

$$B.C.2: \quad z = h: \quad D_\infty\frac{\partial C(h,t)}{\partial z} = 0. \qquad (31)$$

At the macroscopic scale the diffusing DNA molecule appears as a mathematical point, and we simplify the notation from z_0 to z. Equations (28–31) can be cast in the dimensionless form

$$\frac{\partial\xi}{\partial\tau} = \left(\frac{1}{Da}\right)\frac{\partial^2\xi}{\partial\eta^2}, \qquad (32)$$

$$\xi(\eta,0) = 1, \qquad (33)$$

$$\frac{\partial\xi}{\partial\eta}(0,\tau) = Da\,\xi(0,\tau), \qquad (34)$$

$$\frac{\partial\xi}{\partial\eta}(1,\tau) = 0, \qquad (35)$$

where

$$\xi = \frac{C}{C_0}; \quad \eta = \frac{z}{h}; \quad \tau = \frac{\overline{k}}{h}t; \quad Da = \frac{\overline{k}h}{D_\infty}. \qquad (36)$$

The symbol η here denotes a new dimensionless coordinate based on the total thickness h of the liquid layer, which is the pertinent macroscopic length scale.

Numerical Solution

Equations (1–8) were implemented in a C program to compute the reaction rate constant of surface hybridization as a function of molecular orientation. The microscopic and macroscopic problems were solved using finite differences.

RESULTS

Calculation of Orientation-Dependent Reaction Rate Constant

The rate of hybridization depends on the distance of target DNA from the surface and its orientation relative to the immobilized probe DNA. As the target DNA rotates, the average distance of the reactive nucleotides from their complementary counterparts on the surface changes according to Eq. (6) affecting the numerical values of the reaction rate constant (Eq. 7).
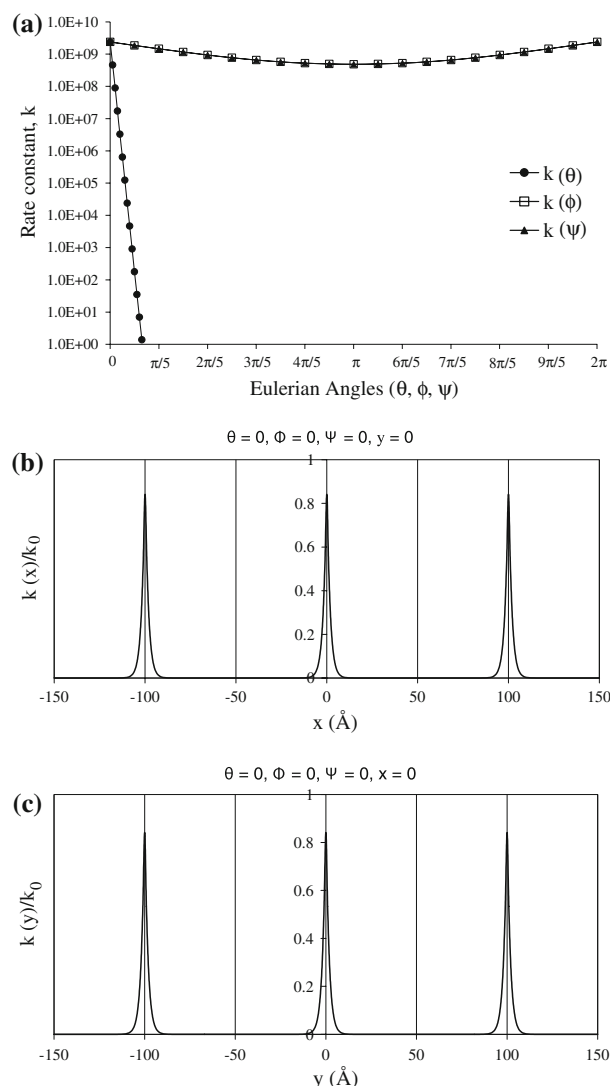
(a)

(b) θ = 0, Φ = 0, Ψ = 0, y = 0

(c) θ = 0, Φ = 0, Ψ = 0, x = 0

FIGURE 2. Dependence of rate constant on *x, y, θ, φ,* and *ψ*. (a) Dependence of rate constant on *θ* (for *φ* = *ψ* = *x* = *y* = 0; *z* = *r*g), *φ* (for *θ* = *ψ* = *x* = *y* = 0; *z* = *r*g), and *ψ* (for *φ* = *θ* = *x* = *y* = 0; *z* = *r*g) for *N* = 500, *N*r = 5 and *k*0 = 2.4 × 10⁹. (b) Dependence of rate constant on *x* (*θ* = *φ* = *ψ* = *y* = 0; *z* = *r*g). (c) Dependence of rate constant on *y* (*θ* = *φ* = *ψ* = *y* = 0; *z* = *r*g).

However, all orientations are not equally important. As shown in Fig. 2a, the reaction rate constant, $k_{config}(x_0, y_0, \theta, \phi, \psi)$ depends very strongly on θ and only weakly on ϕ and ψ. This result reflects the fact that θ controls whether the reactive site faces the surface, and therefore, determines the distance between the complementary nucleotides between target and probe DNA. On the other hand, ϕ and ψ describe rotation of the reactive patch around the axis of the molecule and do not affect the internucleotide distance very strongly. Therefore, the problem can be significantly simplified by averaging k over all ϕ and ψ angles between 0 and 2π.
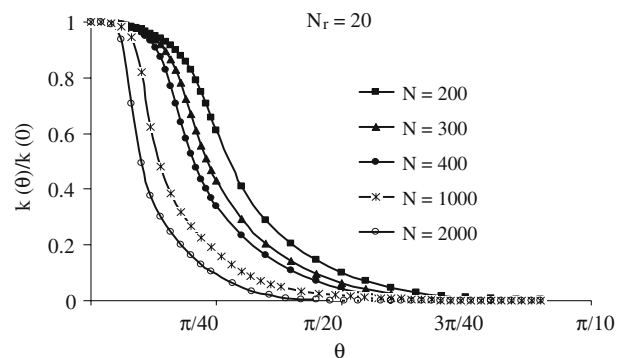

FIGURE 3. Dependence of hybridization rate constant on target DNA orientation. $k(\theta)$ was calculated as a function of θ for target DNA length ranging from 200 to 2000 nucleotides and binding site comprised of 20 nucleotides. $k(\theta)$ for each DNA has been normalized to $k(\theta = 0)$.

In addition to the orientation of the target DNA in solution, the value of the kinetic constant depends on the position of probe DNA on the surface. To simplify the calculations we assume that each probe DNA molecule occupies one unit cell and that all DNA molecules assume the same surface orientation (these assumptions are equivalent to a well-defined monomolecular layer of probe DNA). When there is complete overlap between the binding site of the target DNA with the complementary nucleotides of the probe ($x = 0$, $y = 0$, $\theta = 0$, $\phi = 0$, $\psi = 0$) the reaction rate constant is maximum. Since k is an exponential function of the average distance between complementary nucleotides in the target and probe DNA (Eq. 7), small deviations of the target DNA in the x- or y-direction result in significant decrease in the rate of reaction. The uniform distribution of unit cells on the surface implies that k is a periodic function of x and y (Figs. 2b, c). This spatial periodicity allows calculation of an average reactivity over the whole surface by averaging over all x and y in a single cell. After averaging over all x, y, ϕ, and ψ we obtained $k(\theta)$ (Eq. 8).

The Hybridization Rate is a Strong Function of Target DNA Orientation and Size

Next we calculated the reaction rate constant $k(\theta)$ as a function of target DNA orientation, θ and size, N (Fig. 3). For θ approaching zero there is complete overlap between the complementary sequences of target and probe DNA and $k(\theta)$ is maximum. The value of $k(\theta)$ decreases with increasing θ, approaching zero when θ is between $\pi/20$ and $3\pi/40$. For intermediate deviations from the optimum orientation ($0 < \theta < 3\pi/40$) $k(\theta)$ depends on the size of target DNA, significantly decreasing with increasing DNA length. This result possibly reflects the effect of DNA size on d_{ijk},

which in turn strongly affects the reaction rate. It also shows that only a small number of molecular configurations $(0 < \theta < 3\pi/40)$ contribute significantly to binding.

Microscopic Problem: DNA Concentration Profiles and Average Surface Reactivity

The orientation of target DNA is most important in a thin fluid layer very close to the surface-immobilized probe DNA. In this region, termed the reaction zone, molecular structure controls the distance of each nucleotide from its complementary counterpart on the surface, which in turn determines the rate of hybridization. In the reaction zone, loss of DNA from solution due to hybridization is compensated by a constant flux of DNA molecules from the bulk, thus maintaining the compartment at pseudo-steady state.

Based on these assumptions we formulated the microscopic problem shown in Eqs. (18–21) and in dimensionless form in Eqs. (22–27). Using the values of $k(\theta)$ calculated above, we solved this set of equations to obtain the concentration of target DNA, ξ as a function of dimensionless distance from the surface, η (Fig. 4). For η higher than about 2 or a distance twice the radius of gyration of the target DNA, ξ is a linear function of η and independent of molecular orientation, θ (e.g., $\xi(3,0) = \xi(3,\pi) = \xi(3,\theta)$). For shorter distances, $\eta < 1.5$, there is a strong dependence of concentration on θ. In particular, target DNA with reactive sites facing the surface ($\theta = 0$, complementary

orientation) binds to the probe with high probability and therefore, the DNA concentration at the surface $(\xi(1,0))$ is low in comparison to concentration far away (at 3 molecular radii away) from the surface $(\xi(3,0))$. In contrast, when the reactive site faces opposite to the surface, i.e., for $\theta = \pi$ (noncomplementary orientation), binding to the probe is unlikely and the concentration at the surface is the same as the concentration at $\eta = 3(\xi(1,\pi)/\xi(3,0) = 1)$.

From the solution of the microscopic problem we can calculate an average reaction rate constant, $\overline{k}$ as follows:

$$\frac{\overline{k}r_{\mathrm{g}}}{D_{\infty}} = \frac{1}{\xi_{\mathrm{ext}}(\eta = 1)} \tag{37}$$

where $\xi_{\mathrm{ext}}(\eta = 1)$ is the value of the average dimensionless concentration that is calculated as the intercept of the linear extrapolation of the linear curve ($\xi(\eta)$ for $\eta > 2$) to $\eta = 1$ (Fig. 4; see Appendix A for derivation). With the average reactivity at hand we can now solve the macroscopic problem to calculate the concentration of hybridized DNA as a function of time.

Macroscopic Problem: Kinetics of Hybridization

The values of $\overline{k}$ are used in the solution of the macroscopic problem (Eqs. 28–36) to calculate the rate of binding of target DNA to the surface for different values of Damköhler number, Da, the dimensionless number representing the relative rate of reaction over diffusion. The Damköhler number was varied by changing k_0, which is a measure of affinity of target for probe DNA. Then we solved the microscopic problem (Eqs. 22–27) to calculate the average reaction rate $\overline{k}$, which was subsequently used to solve the macroscopic problem (Eqs. 32–36).

Typically, the hybridization sequence is comprised of about 20 bases that are complementary between the probe and target DNAs. For a target DNA comprising of 200 bases the fractional binding to the surface is plotted as a function of time for different values of the Damköhler number (Fig. 5). For early times, the fraction of DNA that hybridizes to the surface increases linearly, eventually reaching a plateau. When the rate of reaction is comparable to the rate of diffusion $(Da = 1.2)$, the time to hybridize 50% of the DNA (half-time) is about 12 h. As expected, when the reaction rate is much faster than the rate of diffusion $(Da = 12)$, the binding rate increases so that half of the DNA is bound within approximately 3.5 h. Further increasing $Da (Da = 114)$ does not improve the hybridization rate, suggesting that for this value of Da the overall rate of binding to the surface is diffusion limited.
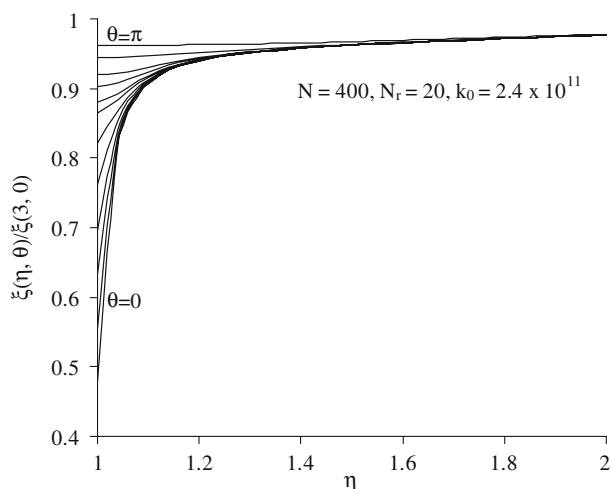

FIGURE 4. The target DNA concentration profile close to the surface strongly depends on molecular orientation. Target DNA dimensionless concentration profile for orientations ranging from complementary ($\theta = 0$) to noncomplementary ($\theta = \pi$). Target DNA of 400 nucleotides with 20 nucleotide binding site was chosen for illustration ($k_0 = 2.4 \times 10^{11}$). The dimensionless concentration was normalized to that at $\eta = 3$ (or $z = 3r_{\mathrm{g}}$) where the concentration of DNA no longer depends on orientation.
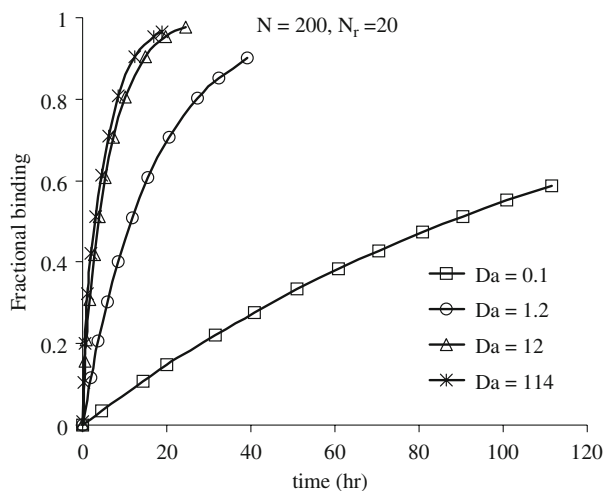
FIGURE 5. Effect of Damköhler number (*Da*) on hybridization kinetics. Fractional binding as a function of time for target DNA of 200 nucleotides containing a 20 nucleotide reactive site. Each curve represents the kinetics for the indicated Damköhler number obtained by varying k_0 between 2.4×10^7 and 2.4×10^{10}.
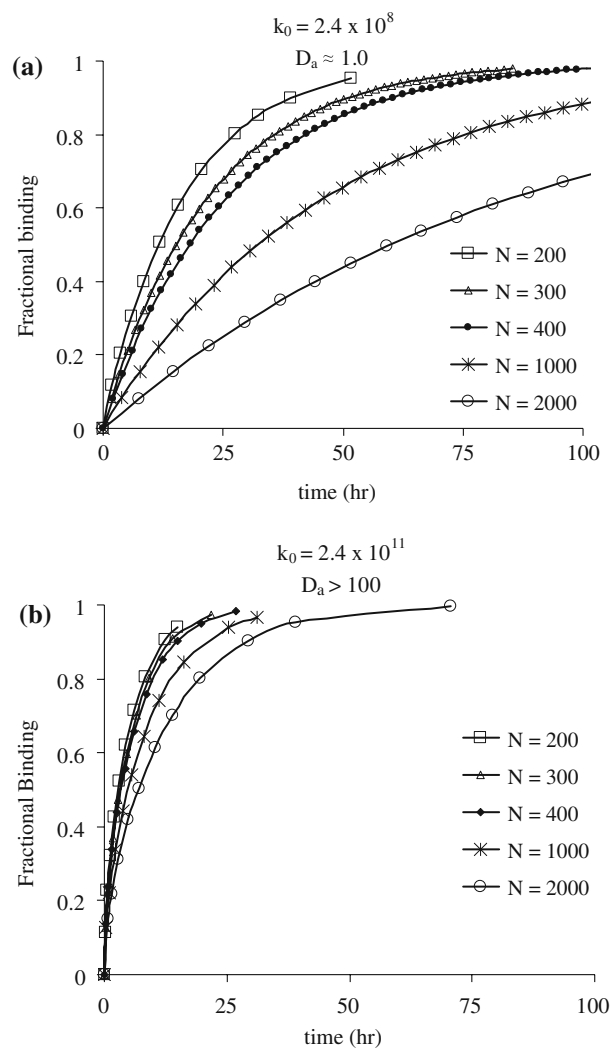

FIGURE 6. Effect of target DNA size on hybridization kinetics. Fractional binding as a function of time for target DNA ranging from 200 to 2000 nucleotides containing a 20 nucleotide reactive site. k_0 was set at (a) 2.4×10^8 or (b) 2.4×10^{11} to yield Damköhler number of ≈ 1 or ≈ 1000, respectively.

The Rate of Hybridization Depends Strongly on the Size of Target DNA

Since the internucleotide distance, d_{ijk} and the therefore, the reaction rate constant, $k(\theta)$ depend on the size of target DNA (Fig. 3), we examined the dependence of hybridization kinetics for varying DNA lengths between 200 and 2000 bases. When the affinity of probe and target DNA is moderate so that the reaction and diffusion rates are comparable ($Da \approx 1$), the rate of hybridization is a very strong function of the size of target DNA, decreasing for larger DNA molecules (Fig. 6a). For example, the half-time for hybridization increases from 12 h to more than 60 h when the size of target DNA increases from 200 to 2000 bases. These results reflect the strong dependence of the reaction rate constant $k(\theta)$ on the size of target DNA. In contrast, when the affinity of target DNA for the probe is very high ($Da \gg 1$; diffusion-limited regime), the rate of binding is a weak function of DNA length (Fig. 6b), possibly reflecting the weak dependence of the diffusion coefficient on DNA size ($D_\infty \sim 1/N^{1/3}$).

Hybridization of Short DNA Targets is Diffusion Limited but Hybridization of Long DNA Targets is Reaction Limited

At early times the concentration of target DNA adjacent to the surface is high and readily available for binding. In this region binding increases linearly with time, suggesting that hybridization is limited by the rate of reaction (Fig. 7a). When the target DNA close to the surface is depleted the binding rate decreases and hybridization scales with the square root of time, suggesting that hybridization becomes diffusion limited. The switch from reaction-limited to diffusion-limited hybridization occurs at a time that depends on the value of the Damköhler number, *Da*, and the size of target DNA.

Specifically, binding switches from being kinetically limited to being diffusion limited at a time that increases with decreasing *Da* (Fig. 7a). For a 200 bp DNA target, as *Da* decreases from ~100 to 10, 1, or 0.1, hybridization becomes diffusion limited at approximately 1 min, 28 min, 4.7 h, or 35 h, respectively. These calculations suggest that for the duration of the typical microarray hybridization experiment (overnight to 24 h) hybridization is—for the most
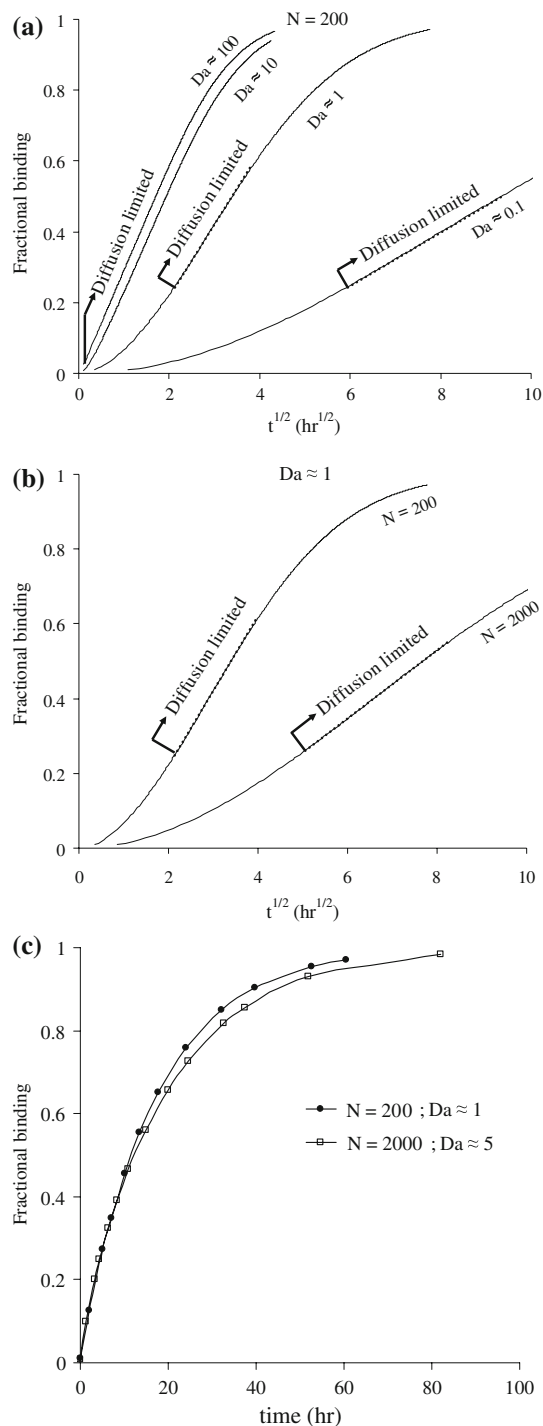
(a)

(b)

(c)

FIGURE 7. **Hybridization is diffusion limited for short DNA targets but kinetically limited for long ones. Fractional binding is plotted as a function of the square root of time ($t^{1/2}$) for target DNA of 200 or 2000 nucleotides containing a 20-nucleotide reactive site. The indicated values of the Damköhler number were obtained by varying the affinity constant k_0. (a) $N = 200$ and k_0 between 2.4×10^7 and 2.4×10^{10}. (b) $k_0 = 2.4 \times 10^8$ ($Da \approx 1$) for $N = 200$ or 2000. (c) Fractional binding as a function of time. The parameters used were $k_0 = 2.4 \times 10^8$ for $N = 200$ and $k_0 = 2.4 \times 10^9$ for $N = 2000$ and yielded $Da \approx 1$ and 5, respectively.**

part—diffusion limited for very high Da ($Da \approx 100$ or 10) but kinetically limited for very low Da ($Da \approx 0.1$). For $Da \approx 1$, hybridization is affected by the surface reaction rate for a significant fraction of the experiment's time (4.7 h) before the diffusion resistance dominates the overall rate.

Next, we computed the time when hybridization becomes diffusion limited for short ($N = 200$ bp) and long DNA targets ($N = 2000$). Figure 7b shows that for the same value of the affinity parameter k_0 ($k_0 = 2.4 \times 10^8$; $Da \approx 1$), hybridization of a 2000-nucleotide target becomes diffusion controlled after 25 h as compared to 4.7 h for a 200-nucleotide target. These calculations suggest that for short targets the reaction rate is fast and hybridization becomes diffusion limited early on but long targets are kinetically limited for the duration of a microarray experiment.

Interestingly, the hybridization rate of a low affinity, 200-nucleotide DNA target ($k_0 = 2.4 \times 10^8$ yielding $Da \approx 1$) is very similar to that of a high affinity, 2000-nucleotide long target ($k_0 = 2.4 \times 10^9$ yielding $Da \approx 5$) (Fig. 7c). This result reflects the strong dependence of the surface binding rate on target DNA size, which stems from the dependence of the reaction rate constant on molecular orientation ($k(\theta)$). It suggests that in the presence of a wide size distribution of DNA targets it may be very difficult to distinguish between specific binding (high k_0) of long sequences and nonspecific binding (low k_0) of short ones.

DISCUSSION

Although DNA microarrays have revolutionized our way of thinking about modern biology and medicine, the technology still faces some conceptual and technical problems including noise, standardization of experimental procedures, and methods of analysis, which must be resolved before microarrays can be used reliably and quantitatively. In this regard, understanding the underlying physical and chemical behavior of the process of surface hybridization is necessary to design efficient and accurate microarray devices.

In this communication, we developed a mathematical framework to analyze the kinetics of DNA hybridization. We modeled DNA hybridization as a function of distance of each nucleotide from its complementary counterpart, which in turn depends on the position of the reactive nucleotides on the target molecule. By accounting for the physical distance of the reactive sites of target and probe DNAs we take into account the effect of molecular orientation on the kinetics of hybridization. Since nucleotides hybridize only when the two complementary strands are in close

proximity and in anti-parallel orientation the rate of reaction depends strongly on the orientation of the reactive site of the target DNA with respect to the immobilized probe. Our calculations show that the reaction rate constant of hybridization is a strong function of the target DNA orientation. Small deviation from the orientation that corresponds to perfect match between target and probe ($\theta = 0$) results in decreased reaction rate constant. These results show that our kinetic model captures the dependence of hybridization on the relative orientation of target and probe DNA and therefore, it predicts the rate of binding as a function of target DNA size.

In our treatment, the reactive site was taken to be small ($N_r = 20$ nt) compared the radius of the sphere or between 1 and 10% of the total number of nucleotides (N varied between 200 and 2000 nt). In this case, the reactive patch is almost linear and can come in contact with the immobilized linear probe on the surface. In addition to this physical constraint, other limitations may also arise for longer reactive sites. For example, a reactive site of 200 nt would not bind at once but rather in steps. Binding of the first few nucleotides is expected to constrain the alignment of the remaining complementary bases and increase the rate of subsequent binding steps. Therefore, binding of long reactive sites would likely require a kinetic model that accounts for this "zipping" reaction mechanism.[14] Although the "zipping" model would likely change the reaction rate, binding of the first nucleotides would still depend on molecular orientation θ, and therefore, our conclusions on the importance of target DNA orientation may be valid even for longer reactive sites.

Our computations predict that as the length of target DNA increases the rate of hybridization decreases. Hybridization of long targets continues almost at a constant rate long after short target hybridization is complete. For the parameter values used in the model, the half-time of hybridization for a 200 bp target DNA was approximately 12 h as compared to 18 h for a 400 bp and more than 60 h for 2000 bp DNA. These results suggest that for accurate quantitation of gene expression and comparison between different genes products, the lengths of the target cDNAs should be very similar to ensure similar hybridization kinetics. Preferably, the length of cDNAs should be 200 bp or shorter since binding is significantly faster for shorter molecules. Indeed some microarray manufacturers designed gene-specific primers or developed protocols for cDNA or cRNA fragmentation via treatment with nucleases, radicals, or shear force to yield 50–200 bp fragments.[35] The rationale for decreasing the target DNA size was to reduce the likelihood of self-hybridization that may

mask the binding site. However, our computations show that smaller target DNAs also yield faster hybridization kinetics allowing for shorter reaction times, thereby reducing the likelihood of background noise due to nonspecific binding.

The relative significance of reaction and diffusion has been debated in recent literature.[5,11,21,38] While, some suggested that hybridization may be reaction limited,[11] others showed that the hybridization is reaction limited at early times when the target DNA concentration is high, but becomes diffusion limited at longer times as the target is consumed.[21,39] Experimental studies showed that continuous mixing or convective flow improved the rate and intensity of hybridization signals, suggesting that diffusion is indeed a limiting factor in surface hybridization.[5,40,55,56]

In addition to translational diffusion, our model accounts for rotational diffusion and its effect on surface reaction and suggests that the relative contribution of these processes may depend on the size of target DNA. Our calculations showed that for short targets the reaction rate is fast and hybridization is diffusion limited but long targets are kinetically limited for the duration of the typical microarray experiment. This result suggests that mixing or convective flow will have no effect on the hybridization rate of long DNA targets. These strategies are more likely to enhance hybridization of short targets, which are limited by the rate of diffusion. In addition, we showed that short and low affinity targets may hybridize with a similar rate as long targets of high affinity, suggesting that the results of microarray experiments may be hampered by nonspecific binding or high background noise. As a result for a wide size distribution of DNA targets, the signal intensity of each spot may not reflect the starting DNA target concentration in solution.

Based on these results, we recommend that microarray experiments are performed under the following conditions. (i) Employ short DNA targets that can be obtained either by fragmentation or reverse transcription with gene-specific primers. Shortening would eliminate the kinetic limitation and maximize specificity by eliminating the dependence of hybridization on molecular size. As a result, signal intensity should correlate better with the starting target concentration in solution as a low signal may be more likely to represent low target concentration in the bulk rather than inefficient binding due to large DNA target size. (ii) Application of continuous mixing or convective flow to overcome the diffusion limitation of short DNA targets. These operating conditions would enhance the hybridization rate, thereby allowing for shorter reaction times, which would ultimately decrease background noise and improve accuracy.

The present model is valid when surface saturation is low and reverse hybridization rate does not significantly affect the overall reaction rate. However, experimentally derived association constants range between 10^4 and 10^6 M^{-1} s^{-1}, while dissociation constants are much lower 10^{-5}–10^{-1} s^{-1},[3,62] suggesting that dissociation would be important only for high surface coverage or very long incubation times. Since microarrays are usually run with probe saturation values of much less than 5%,[3] our results should be generally applicable. Finally, the present model can be extended to account for sequence of the binding site as well as nearest neighbor interactions[48] by incorporating thermodynamic arguments of base-pair interactions in the formulation of the reaction rate constant. Such treatment would predict the effect of DNA sequence—including mismatches, e.g., G-C vs. G-A—on hybridization kinetics, thereby predicting the extent of nonspecific binding of targets to partially complementary probes.

In summary, we presented a comprehensive mathematical model that describes the kinetics of DNA hybridization. We proposed a novel way to calculate the reaction rate constant based on the physical distance of complementary nucleotides and account for orientation of target DNA relative to the immobilized probe. In addition, our model describes the translational and rotational diffusion of DNA molecules as they travel to the surface and accounts for the surface reaction at the boundary condition. The model predicts the effect of DNA orientation on reaction affinity and the effects of target DNA length on hybridization rate. Our results suggest changes in the conditions of microarray experiments to increase the accuracy of gene expression levels and enable comparison among different genes in the same array. Therefore, development of experimental conditions based on a better understanding of the underlying physical and chemical steps of surface hybridization may reduce the errors and increase the accuracy and consistency of microarray measurements.

APPENDIX A

At $z = r_g$ the flux, β, entering the microscopic diffusion layer is equal to the rate of reaction:

$$D_\infty \frac{\partial C}{\partial z}\bigg|_{z=r_g} = \beta D_\infty = \overline{k}C|_{z=r_g} \tag{A1}$$

Note that the flux, β entering the reaction zone layer is the same as the flux far from the surface ($z \to \infty$) (see Eq. 20). From Eq. (27) we substitute the dimensionless

variables $\xi = C/\beta r_g$ and $\eta = z/r_g$ into Eq. (A1) to obtain:

$$\frac{\overline{k}r_g}{D_\infty} = \frac{1}{\xi|_{\eta=1}} \tag{A2}$$

The value of $\xi|_{\eta=1}$ is obtained as the intercept of the linear part of $\xi(\eta)$ curve (Fig. 4) to $\eta = 1$.

REFERENCES

[1]Allison, D. B., X. Cui, G. P. Page, and M. Sabripour. Microarray data analysis: from disarray to consolidation and consensus. *Nat. Rev. Genet*. 7(1):55–65, 2006. doi:10.1038/nrg1749.

[2]Ames, J. S., and F. D. Murnaghan. Theoretical Mechanics: An Introduction to Mathematical Physics. New York: Dover, pp. 80–82, 1958.

[3]Benn, J. A., J. Hu, B. J. R. C. Hogan Fry, L. D. Samson, and T. Thorsen. Comparative modeling and analysis of microfluidic and conventional DNA microarrays. *Anal. Biochem*. 348(2):284–293, 2006. doi:10.1016/j.ab.2005.10.033.

[4]Bird, R. B., W. E. Stewart, and E. N. Lightfoot. Transport Phenomena. 2nd ed. New York: John Wiley & Sons, 2007.

[5]Borden, J. R., C. J. Paredes, and E. T. Papoutsakis. Diffusion, mixing, and associated dye effects in DNA-microarray hybridizations. *Biophys. J*. 89(5):3277–3284, 2005. doi:10.1529/biophysj.105.067934.

[6]Brenner, H. The slow motion of a sphere through a viscous fluid towards a plane surface. *Chem. Eng. Sci*. 16:242–251, 1961. doi:10.1016/0009-2509(61)80035-3.

[7]Brenner, H. Coupling between the translational and rotational Brownian motions of rigid particles of arbitrary shape. *J. Colloid Interface Sci*. 23:407–436, 1967. doi:10.1016/0021-9797(67)90185-3.

[8]Brenner, H., and D. W. Condiff. Transport mechanics in systems of orientable particles. 3. Arbitrary particles. *J. Colloid Interface Sci*. 41(2):228–272, 1972. doi:10.1016/0021-9797(72)90111-7.

[9]Brenner, H., and D. W. Condiff. Transport mechanics in systems of orientable particles .4. Convective transport. *J. Colloid Interface Sci*. 47(1):199–264, 1974. doi:10.1016/0021-9797(74)90093-9.

[10]Brown, P. O., and D. Botstein. Exploring the new world of the genome with DNA microarrays. *Nat. Genet*. 21(1 Suppl):33–37, 1999. doi:10.1038/4462.

[11]Chan, V., D. J. Graves, and S. E. McKenzie. The biophysics of DNA hybridization with immobilized oligonucleotide probes. *Biophys. J*. 69:2243–2255, 1995.

[12]Claeys, T. L., and J. F. Brady. Lubrication singularities of the grand resistance tensor for 2 arbitrary particles. *Physicochem. Hydrodyn*. 11(3):261–293, 1989.

[13]Condiff, D. W., and J. S. Dahler. Brownian motion of polyatomic molecules: the coupling of rotational and translational motions. *J. Chem. Phys*. 44(10):3988–4004, 1966. doi:10.1063/1.1726561.

[14]Craig, M. E., D. M. Crothers, and P. Doty. Relaxation kinetics of dimer formation by self complementary oligonucleotides. *J. Mol. Biol*. 62(2):383–401, 1971. doi:10.1016/0022-2836(71)90434-7.

[15] Dai, H., M. Meyer, S. Stepaniants, M. Ziman, and R. Stoughton. Use of hybridization kinetics for differentiating specific from non-specific binding to oligonucleotide microarrays. *Nucleic Acids Res*. 30(16):e86, 2002. doi:10.1093/nar/gnf085.

[16] Deeb, G., M. R. Baer, D. P. Gaile, S. N. Sait, M. Barcos, M. Wetzler, J. M. Conroy, N. J. Nowak, J. K. Cowell, and R. T. Cheney. Genomic profiling of myeloid sarcoma by array comparative genomic hybridization. *Genes Chromosomes Cancer* 44(4):373–383, 2005. doi:10.1002/gcc.20239.

[17] Demeter, J., C. Beauheim, J. Gollub, T. Hernandez-Boussard, H. Jin, D. Maier, J. C. Matese, M. Nitzberg, F. Wymore, Z. K. Zachariah, P. O. Brown, G. Sherlock, and C. A. Ball. The Stanford Microarray Database: implementation of new analysis tools and open source release of software. *Nucleic Acids Res*. 35(Database issue):D766–770, 2007. doi:10.1093/nar/gkl1019.

[18] DeRisi, J. L., V. R. Iyer, and P. O. Brown. Exploring the metabolic and genetic control of gene expression on a genomic scale. *Science* 278(5338):680–686, 1997. doi:10.1126/science.278.5338.680.

[19] DeRisi, J., L. Penland, P. O. Brown, M. L. Bittner, P. S. Meltzer, M. Ray, Y. Chen, Y. A. Su, and J. M. Trent. Use of a cDNA microarray to analyse gene expression patterns in human cancer. *Nat. Genet.* 14(4):457–460, 1996. doi:10.1038/ng1296-457.

[20] Erickson, D., D. Li, and U. J. Krull. Modeling of DNA hybridization kinetics for spatially resolved biochips. *Anal. Biochem.* 317(2):186–200, 2003. doi:10.1016/S0003-2697(03)00090-3.

[21] Gadgil, C., A. Yeckel, J. J. Derby, and W. S. Hu. A diffusion-reaction model for DNA microarray assays. *J. Biotechnol.* 114(1–2):31–45, 2004. doi:10.1016/j.jbiotec.2004.05.008.

[22] Goldstein, H. Classical Mechanics. 3rd ed. San Francisco: Addison Wesley, 2002.

[23] Golub, T. R., D. K. Slonim, P. Tamayo, C. Huard, M. Gaasenbeek, J. P. Mesirov, H. Coller, M. L. Loh, J. R. Downing, M. A. Caligiuri, C. D. Bloomfield, and E. S. Lander. Molecular classification of cancer: class discovery and class prediction by gene expression monitoring. *Science* 286(5439):531–537, 1999. doi:10.1126/science.286.5439.531.

[24] Graves, D. J. Powerful tools for genetic analysis come of age. *Trends Biotechnol.* 17(3):127–134, 1999. doi:10.1016/S0167-7799(98)01241-4.

[25] Happel, J., and H. Brenner. Low Reynolds Number Hydrodynamics: With Special Applications to Particulate Media. Boston, MA: M. Nijhoff/Kluwer, 1983.

[26] Held, G. A., G. Grinstein, and Y. Tu. Modeling of DNA microarray data by using physical properties of hybridization. *Proc. Natl. Acad. Sci. USA* 100(13):7575–7580, 2003. doi:10.1073/pnas.0832500100.

[27] Irizarry, R. A., B. M. Bolstad, F. Collin, L. M. Cope, B. Hobbs, and T. P. Speed. Summaries of affymetrix GeneChip probe level data. *Nucleic Acids Res.* 31(4):e15, 2003. doi:10.1093/nar/gng015.

[28] Iyer, V. R., M. B. Eisen, D. T. Ross, G. Schuler, T. Moore, J. C. F. Lee, J. M. Trent, L. M. Staudt, J. Hudson, Jr., M. S. Boguski, D. Lashkari, D. Shalon, D. Botstein, and P. O. Brown. The transcriptional program in the response of human fibroblasts to serum [see comments]. *Science* 283(5398):83–87, 1999. doi:10.1126/science.283.5398.83.

[29] Koria, P., and S. T. Andreadis. Epidermal morphogenesis: the transcriptional program of human keratinocytes during stratification. *J. Invest. Dermatol.* 126(8):1834–1841, 2006. doi:10.1038/sj.jid.5700325.

[30] Koria, P., D. Brazeau, K. Kirkwood, P. Hayden, M. Klausner, and S. T. Andreadis. Gene expression profile of tissue engineered skin subjected to acute barrier disruption. *J. Invest. Dermatol.* 121(2):368–382, 2003. doi:10.1046/j.1523-1747.2003.12364.x.

[31] Lashkari, D. A., J. L. DeRisi, J. H. McCusker, A. F. Namath, C. Gentile, S. Y. Hwang, P. O. Brown, and R. W. Davis. Yeast microarrays for genome wide parallel genetic and gene expression analysis. *Proc. Natl. Acad. Sci. USA* 94(24):13057–13062, 1997. doi:10.1073/pnas.94.24.13057.

[32] Li, S., J. Lao, B. P. Chen, Y. S. Li, Y. Zhao, J. Chu, K. D. Chen, T. C. Tsou, K. Peck, and S. Chien. Genomic analysis of smooth muscle cells in 3-dimensional collagen matrix. *FASEB J.* 17(1):97–99, 2003.

[33] Li, C., and W. H. Wong. Model-based analysis of oligonucleotide arrays: expression index computation and outlier detection. *Proc. Natl. Acad. Sci. USA* 98(1):31–36, 2001. doi:10.1073/pnas.011404098.

[34] Liu, Y., and C. B. Rauch. DNA probe attachment on plastic surfaces and microfluidic hybridization array channel devices with sample oscillation. *Anal. Biochem.* 317(1):76–84, 2003. doi:10.1016/S0003-2697(03)00051-4.

[35] Mehlmann, M., M. B. Townsend, R. L. Stears, R. D. Kuchta, and K. L. Rowlen. Optimization of fragmentation conditions for microarray analysis of viral RNA. *Anal. Biochem.* 347(2):316–323, 2005. doi:10.1016/j.ab.2005.09.036.

[36] Nitsche, J. M., and H. Brenner. On the formulation of boundary conditions for rigid nonspherical Brownian particles near solid walls: applications to orientation-specific reactions with immobilized enzymes. *J. Colloid Interface Sci.* 138:21–41, 1990. doi:10.1016/0021-9797(90)90177-P.

[37] Nowak, N. J., D. Gaile, J. M. Conroy, D. McQuaid, J. Cowell, R. Carter, M. G. Goggins, R. H. Hruban, and A. Maitra. Genome-wide aberrations in pancreatic adenocarcinoma. *Cancer Genet. Cytogenet.* 161(1):36–50, 2005. doi:10.1016/j.cancergencyto.2005.01.009.

[38] Pappaert, K., H. Ottevaere, H. Thienpont, P. Van Hummelen, and G. Desmet. Diffusion limitation: a possible source for the occurrence of doughnut patterns on DNA microarrays. *Biotechniques* 41(5):609–616, 2006.

[39] Pappaert, K., P. Van Hummelen, J. Vanderhoeven, G. V. Baron, and G. Desmet. Diffusion-reaction modeling of DNA hybridization kinetics on biochips. *Chem. Eng. Sci.* 58(21):4921–4930, 2003. doi:10.1016/j.ces.2002.12.007.

[40] Pappaert, K., J. Vanderhoeven, P. Van Hummelen, B. Dutta, D. Clicq, G. V. Baron, and G. Desmet. Enhancement of DNA micro-array analysis using a shear-driven micro-channel flow system. *J. Chromatogr. A* 1014(1–2):1–9, 2003. doi:10.1016/S0021-9673(03)00715-5.

[41] Parkinson, H., M. Kapushesky, M. Shojatalab, N. Abeygunawardena, R. Coulson, A. Farne, E. Holloway, N. Kolesnykov, P. Lilja, M. Lukk, R. Mani, T. Rayner, A. Sharma, E. William, U. Sarkans, and A. Brazma. ArrayExpress—a public database of microarray experiments and gene expression profiles. *Nucleic Acids Res.* 35(Database issue):D747–750, 2007. doi:10.1093/nar/gkl995.

[42] Parvathy, V. R., S. R. Bhaumik, K. V. Chary, G. Govil, K. Liu, F. B. Howard, and H. T. Miles. NMR structure of a parallel-stranded DNA duplex at atomic resolution. *Nucleic Acids Res.* 30(7):1500–1511, 2002. doi:10.1093/nar/30.7.1500.

[43] Pavlova, A., R. O. Stuart, M. Pohl, and S. K. Nigam. Evolution of gene expression patterns in a model of branching morphogenesis. *Am. J. Physiol.* 277(4 Pt 2): F650–663, 1999.

[44]Perou, C. M., S. S. Jeffrey, M. van de Rijn, C. A. Rees, M. B. Eisen, D. T. Ross, A. Pergamenschikov, C. F. Williams, S. X. Zhu, J. C. Lee, D. Lashkari, D. Shalon, P. O. Brown, and D. Botstein. Distinctive gene expression patterns in human mammary epithelial cells and breast cancers. *Proc. Natl. Acad. Sci. USA* 96(16):9212–9217, 1999. doi:10.1073/pnas.96.16.9212.

[45]Peterson, A. W., R. J. Heaton, and R. M. Georgiadis. The effect of surface probe density on DNA hybridization. *Nucleic Acids Res.* 29(24):5163–5168, 2001. doi:10.1093/nar/29.24.5163.

[46]Peterson, A. W., L. K. Wolf, and R. M. Georgiadis. Hybridization of mismatched or partially matched DNA at surfaces. *J. Am. Chem. Soc.* 124(49):14601–14607, 2002. doi:10.1021/ja0279996.

[47]Rhodes, D. R., J. Yu, K. Shanker, N. Deshpande, R. Varambally, D. Ghosh, T. Barrette, A. Pandey, and A. M. Chinnaiyan. ONCOMINE: a cancer microarray database and integrated data-mining platform. *Neoplasia* 6(1):1–6, 2004.

[48]SantaLucia, J., Jr., H. T. Allawi, and P. A. Seneviratne. Improved nearest-neighbor parameters for predicting DNA duplex stability. *Biochemistry* 35(11):3555–3562, 1996. doi:10.1021/bi951907q.

[49]Shalon, D., S. J. Smith, and P. O. Brown. A DNA microarray system for analyzing complex DNA samples using two-color fluorescent probe hybridization. *Genome Res.* 6(7):639–645, 1996. doi:10.1101/gr.6.7.639.

[50]Spellman, P. T., G. Sherlock, M. Q. Zhang, V. R. Iyer, K. Anders, M. B. Eisen, P. O. Brown, D. Botstein, and B. Futcher. Comprehensive identification of cell cycle-regulated genes of the yeast *Saccharomyces cerevisiae* by microarray hybridization. *Mol. Biol. Cell* 9(12):3273–3297, 1998.

[51]Stillman, B. A., and J. L. Tonkinson. Expression microarray hybridization kinetics depend on length of the immobilized DNA but are independent of immobilization substrate. *Anal. Biochem.* 295(2):149–157, 2001. doi:10.1006/abio.2001.5212.

[52]Tamayo, P., D. Slonim, J. Mesirov, Q. Zhu, S. Kitareewan, E. Dmitrovsky, E. S. Lander, and T. R. Golub. Interpreting patterns of gene expression with self-organizing maps: methods and application to hematopoietic differentiation. *Proc. Natl. Acad. Sci. USA* 96(6):2907–2912, 1999. doi:10.1073/pnas.96.6.2907.

[53]Tinland, B., A. Pluen, J. Sturm, and G. Weill. Persistence length of single stranded DNA. *Macromolecules* 30:5763–5765, 1997. doi:10.1021/ma970381+.

[54]Toronen, P., M. Kolehmainen, G. Wong, and E. Castren. Analysis of gene expression data using self-organizing maps. *FEBS Lett.* 451(2):142–146, 1999. doi:10.1016/S0014-5793(99)00524-4.

[55]Vanderhoeven, J., K. Pappaert, B. Dutta, P. Van Hummelen, and G. Desmet. DNA microarray enhancement using a continuously and discontinuously rotating microchamber. *Anal. Chem.* 77(14):4474–4480, 2005. doi:10.1021/ac0502091.

[56]Vanderhoeven, J., K. Pappaert, B. Dutta, P. Van Hummelen, and G. Desmet. Comparison of a pump-around, a diffusion-driven, and a shear-driven system for the hybridization of mouse lung and testis total RNA on microarrays. *Electrophoresis* 26(19):3773–3779, 2005.

[57]Wang, J. Y., and K. Drlica. Modeling hybridization kinetics. *Math. Biosci.* 183(1):37–47, 2003. doi:10.1016/S0025-5564(02)00221-3.

[58]Weinberger, H. F. A First Course in Partial Differential Equations. New York: Wiley, 1965.

[59]Wen, X., S. Fuhrman, G. S. Michaels, D. B. Carr, S. Smith, J. L. Barker, and R. Somogyi. Large-scale temporal gene expression mapping of central nervous system development. *Proc. Natl. Acad. Sci. USA* 95(1):334–339, 1998. doi:10.1073/pnas.95.1.334.

[60]Whittaker, E. T. A Treatise on the Analytical Dynamics of Particles and Rigid Bodies. 4th ed. New York: Dover, pp. 9–10, 1944.

[61]Yang, Y. H., S. Dudoit, P. Luu, D. M. Lin, V. Peng, J. Ngai, and T. P. Speed. Normalization for cDNA microarray data: a robust composite method addressing single and multiple slide systematic variation. *Nucleic Acids Res.* 30(4):e15, 2002. doi:10.1093/nar/30.4.e15.

[62]Zhang, Y., D. A. Hammer, and D. J. Graves. Competitive hybridization kinetics reveals unexpected behavior patterns. *Biophys. J.* 89(5):2950–2959, 2005. doi:10.1529/biophysj.104.058552.